

## Thermodynamics of PNJL model at zero temperature in a strong magnetic field

Yuan Wang<sup>1</sup> and Xin-Jian Wen<sup>1\*</sup>

*Institute of Theoretical Physics, Shanxi University, Taiyuan, Shanxi 030006, China  
and Collaborative Innovation Center of Extreme Optics, Shanxi University,  
Taiyuan, Shanxi 030006, People's Republic of China*

 (Received 10 January 2022; accepted 12 April 2022; published 29 April 2022)

In this paper, the deconfinement and chiral restoration transitions in a strong magnetic field are realized at zero temperature in the Polyakov Nambu-Jona-Lasinio model. We provide the thermodynamic treatment to mimic the deconfinement phase transition at zero temperature together with the entangled scalar and vector interactions coupled with the Polyakov loop. The magnetic catalysis is found by a rising behavior of the critical chemical potential for the first-order deconfinement phase transition. While the magnetic catalysis on the chiral restoration could convert to inverse magnetic catalysis under the running coupling interaction ansatz. Furthermore, the stronger magnetic field makes the possible quarkyonic phase window to be enlarged under the running coupling interaction.

DOI: [10.1103/PhysRevD.105.074034](https://doi.org/10.1103/PhysRevD.105.074034)

### I. INTRODUCTION

The study of the quantum chromodynamics (QCD) phase diagram attracts a lot of attention theoretically and experimentally [1–4]. The three basic characteristics of QCD, chiral symmetry, quark confinement and asymptotic freedom, play an important role in determining the properties of hadrons and the phase diagram at finite temperature and density. Understanding these aspects could help us to get a better knowledge of the strongly interacting matter.

In the past decades, one powerful lattice QCD was established for  $2 + 1$  flavors and vanishing baryon chemical potential. It is predicted that there is a crossoverlike transition at high temperature from a hadronic phase. However, the situation is less clear for finite chemical potentials due to the well-known difficulty given by the so-called sign problem, which affects lattice calculations [5]. Thus the more work on QCD diagram has to be done in the phenomenological models, which capture the basic physics of QCD itself and are instructive to evaluate the quark mass, the pion mass, and so on. First, the asymptotic freedom indicates the interaction of quarks becomes weaker with decreasing distance and becomes stronger as the separation increases. It can be described by a variational coupling

constant [6] or represented by an density-and-temperature dependent mass of quasiparticle in literature [7–9]. Second, the chiral symmetry breaking was successfully investigated by the Nambu-Jona-Lasinio (NJL) model at finite temperature by the dynamical generation of quark mass, which can act as an order parameter of chiral phase transition [10–16]. Third, the quark confinement as an essential feature of QCD involves nonperturbative properties. The MIT bag model is based on a phenomenological realization of quark confinement. The bag constant is often introduced phenomenologically with the expectation that it simulate nonperturbative corrections [17–19]. At high densities of a good simulation of the compact star, the deconfinement phase transition is expected to take place, which is characterized by a approximately  $Z(3)$  center symmetry breaking. On the other hand, the MIT bag model violates chiral symmetry and the NJL model does not confine quarks. The question has been addressed by the Polyakov Nambu-Jona-Lasinio (PNJL) model, where the quarks interact with the temporal gluon field, represented by the Polyakov loop. The PNJL model had been successfully employed on the investigation of the chiral phase diagram and the confinement-deconfinement transition during a long period [20–24]. Unfortunately, directly taking the zero temperature limit on the Polyakov potential in the conventional version of the PNJL model is infeasible, which will lead to the vanishing of the confinement mechanism. Recently, by introducing a Polyakov-loop dependent coupling interaction, the confinement-deconfinement transition in the PNJL model has been recovered to be operative at the zero temperature regime, which was named as the PNJL0 model [25,26].

\*wenxj@sxu.edu.cn

*Published by the American Physical Society under the terms of the Creative Commons Attribution 4.0 International license. Further distribution of this work must maintain attribution to the author(s) and the published article's title, journal citation, and DOI. Funded by SCOAP<sup>3</sup>.*

The recent investigation of QCD in strong magnetic fields brings a new sight on the whole phase diagram. The typical strength of the strong magnetic fields could be of the order of  $10^{12}$  Gauss on the surface of pulsars. Some magnetars can have even larger magnetic fields as high as  $10^{16}$  Gauss at the surface and  $10^{18}$  Gauss in the interior of certain compact stars. By comparing the magnetic and gravitational energies, the physical upper limit to the total neutron star is of order  $10^{18}$  Gauss [27]. And for the self-bound quark stars, the limit could go higher [28,29]. A realistic profile of the magnetic field distribution inside strongly magnetized neutron stars is proposed that the magnetic fields increase relatively slowly with increasing baryon chemical potential in the polynomial form instead of exponential form [30]. At the large hadron collider energy in CERN, it is estimated to produce a field as large as  $5 \times 10^{19}$  Gauss [31]. Much stronger background fields might have been produced during the cosmological electroweak phase transition [32,33]. The QCD vacuum characterized by the chiral symmetry breaking would be changed by the enhanced quark-antiquark condensate in strong magnetic fields, which leads to a dynamical generation of quark masses. The corresponding mechanism is the famous magnetic catalysis (MC) effect [34]. The inverse magnetic catalysis (IMC) on the (pseudo)critical temperature revealed by the lattice QCD can be realized by the NJL model with a decreasing critical temperature as the magnetic field increases [35–38]. Up to now, the knowledge on QCD phase diagram is mainly achieved at zero/small chemical potential and finite temperature. The phenomenological investigations try to reproduce the lattice result including the (pseudo)critical temperature and quark condensate at low and high temperature. The QCD phase in the region of larger chemical potential and zero temperature has been not well known yet. The aim of the present paper is to investigate the deconfinement and chiral transition at zero temperature by improving the thermodynamics treatment of the PNJL0 model in strong magnetic fields. Of special interest is the effect of the magnetic field on the critical chemical potential, the confinement property dependent on the Polyakov loop at zero temperature.

This paper is organized as follows. In Sec. II, we present the thermodynamics of the magnetized quark matter in SU(2) PNJL0 model. In Sec. III, the numerical results for the chiral symmetry restoration and deconfinement phase transition are shown at zero temperature. The discussions are focused on the magnetic effect on the chiral and the deconfinement transition with the magnetic field independent and dependent coupling constants. The last section is a short summary.

## II. GENERAL FORMALISM OF PNJL0 IN STRONG MAGNETIC FIELDS

Following the work in the SU(2) version of the PNJL model, the Lagrangian density in a strong magnetic field is given by [25,39]

$$\begin{aligned} \mathcal{L}_{\text{PNJL}} = & \bar{\psi}(i\gamma_\mu D^\mu - m)\psi + G_s[(\bar{\psi}\psi)^2 + (\bar{\psi}i\gamma_5\vec{\tau}\psi)^2] \\ & - G_v(\bar{\psi}\gamma_\mu\psi)^2 - U(\Phi, \bar{\Phi}, T). \end{aligned} \quad (1)$$

where  $\psi$  represents a flavor isodoublet ( $u$  and  $d$  quarks) and  $\vec{\tau}$  are isospin Pauli matrices. The coupling of the quarks to the electromagnetic field is introduced by the covariant derivative  $D_\mu = \partial_\mu - ieQA_\mu$ , where  $Q = \text{diag}(q_u, q_d) = \text{diag}(2/3, -1/3)$  is the quark electric charge matrix. The Polyakov potential describes the deconfinement at finite temperature. In literature, the effective potential  $U(\Phi, \bar{\Phi}, T)$  exhibits a phase transition from color confinement to color deconfinement.

At finite temperature, the Polyakov potential depends explicitly on the traced Polyakov loop and its conjugate  $\Phi$  and  $\bar{\Phi}$  [40,41]. In order to obtain the confinement description at zero temperature, we take  $\Phi = \bar{\Phi}$  for the nonzero quark chemical potentials at the mean-field approximation. So the total thermodynamical potential density for the two-flavor quark matter in the mean-field approximation reads

$$\Omega_{\text{PNJL}} = \sum_{i=u,d} \Omega_i + G_s \sigma^2 - G_v \rho^2 + U(\Phi, T), \quad (2)$$

The integral in the effective thermodynamics potential is not convergent. In literature, the Fock-Schwinger proper-time method [42] is applied to a thermal field theory to obtain the exact expression of the effective potential with B-dependent divergent part in the vacuum regularization [43–45]. Another equivalent method is the magnetic field independent vacuum regularization (MFIR), which is widely employed in the recent work [46–52]. In this paper, we adopt the second regularization scheme. The first term  $\Omega_i$  is defined as  $\Omega_i = \Omega_i^{\text{vac}} + \Omega_i^{\text{mag}} + \Omega_i^{\text{med}}$ . The vacuum, the magnetic field, and medium contributions to the thermodynamical potential are [46–48]

$$\Omega_i^{\text{vac}} = \frac{N_c}{8\pi^2} \left[ M^4 \ln \left( \frac{\Lambda + \epsilon_\Lambda}{M} \right) - \epsilon_\Lambda \Lambda (\Lambda^2 + \epsilon_\Lambda^2) \right], \quad (3)$$

$$\Omega_i^{\text{mag}} = -\frac{N_c |q_i e B|^2}{2\pi^2} \left[ \zeta'(-1, x_i) - \frac{1}{2} (x_i^2 - x_i) \ln(x_i) + \frac{x_i^2}{4} \right], \quad (4)$$

$$\Omega_i^{\text{med}} = -\frac{T |q_i e B}{2\pi^2} \sum_{n_i=0}^{\infty} \alpha_{n_i} \int_0^{\infty} (z_\Phi^+ + z_\Phi^-) dp. \quad (5)$$

where the quantity  $\epsilon_\Lambda$  is defined as  $\epsilon_\Lambda = \sqrt{\Lambda^2 + M^2}$  and  $x_i = \frac{M_i^2}{2|q_i|B}$  is dimensionless. The spin degeneracy factor  $\alpha_n = 2 - \delta_{n0}$  is 1 for the lowest Landau level (LLL) and 2 for otherwise higher Landau levels. The ultraviolet divergence in the vacuum part  $\Omega_i^{\text{vac}}$  of the thermodynamical potential is removed by the momentum cutoff. The partition function densities  $z_\Phi^\pm$  are evaluated by the color traces [39]

$$z_{\Phi}^+ = \ln\{1 + 3(\bar{\Phi} + \Phi e^{-\frac{E_i + \tilde{\mu}_i}{T}})e^{-\frac{E_i + \tilde{\mu}_i}{T}} + e^{-3\frac{E_i + \tilde{\mu}_i}{T}}\}, \quad (6)$$

$$z_{\Phi}^- = \ln\{1 + 3(\Phi + \bar{\Phi} e^{-\frac{E_i - \tilde{\mu}_i}{T}})e^{-\frac{E_i - \tilde{\mu}_i}{T}} + e^{-3\frac{E_i - \tilde{\mu}_i}{T}}\}. \quad (7)$$

Only  $z_{\Phi}^-$  would survive at zero temperature, which produces a traditional step function in the medium term as [46,48]

$$\begin{aligned} \Omega_i^{\text{med}} &= -\frac{|q_i|eB}{2\pi^2} \int_0^{p_z^F} 3(\tilde{\mu}_i - E_{ni}) \\ &= -\frac{N_c |q_i| eB}{4\pi^2} \sum_{n_i=0}^{n_i^{\text{max}}} \alpha_{n_i} \left\{ \tilde{\mu}_i \sqrt{\tilde{\mu}_i^2 - M_{ni}^2} - M_{ni}^2 \right. \\ &\quad \left. \times \ln \left[ \frac{\tilde{\mu}_i + \sqrt{\tilde{\mu}_i^2 - M_{ni}^2}}{M_{ni}} \right] \right\}, \end{aligned} \quad (8)$$

where  $M_{ni} = \sqrt{M_i^2 + 2n|q_i|eB}$  and the color degenerate factor 3 is recovered once more due to the decouple of the color interaction with the Polyakov potential.

By minimizing the thermodynamical potential with respect to the quark condensate  $\sigma_i$  and the Polyakov loop  $\Phi$ , we can have a set of the coupled gap equations [14,25]

$$\frac{\partial P}{\partial \sigma} = 0, \quad \frac{\partial P}{\partial \tilde{\mu}} = 0, \quad \frac{\partial P}{\partial \Phi} = 0. \quad (9)$$

Therefore, we can have an equivalent system of non-interacting quark with the constitute dynamical mass  $M$  and renormalized chemical potential  $\tilde{\mu}$  [14].

$$M_i = m_{i0} - 2G_s \sigma_i. \quad (10)$$

$$\tilde{\mu}_i = \mu_i - 2G_v \rho_i. \quad (11)$$

In our work, the isospin symmetry is assumed and we have  $M_u = M_d = M$ . At zero temperature, the occupied Landau levels have the maximum value

$$n_i^{\text{max}} = \frac{\tilde{\mu}_i^2 - M^2}{2|q_i|eB}. \quad (12)$$

The second term in the Eq. (2) is the contribution from the quark condensate  $\sigma = \sum_{i=u,d} \sigma_i$ . The condensation contribution from the quark with flavor  $i$  is

$$\sigma_i = \sigma_i^{\text{vac}} + \sigma_i^{\text{mag}} + \sigma_i^{\text{med}}. \quad (13)$$

The terms  $\sigma_i^{\text{vac}}$ ,  $\sigma_i^{\text{mag}}$ , and  $\sigma_i^{\text{med}}$  represent the vacuum, the magnetic field, and medium contributions to the quark condensation, respectively as following [47,48],

$$\sigma_i^{\text{vac}} = -\frac{MN_c}{2\pi^2} \left[ \Lambda \sqrt{\Lambda^2 + M^2} - M^2 \ln \left( \frac{\Lambda + \sqrt{\Lambda^2 + M^2}}{M} \right) \right], \quad (14)$$

$$\begin{aligned} \sigma_i^{\text{mag}} &= -\frac{M|q_i|eBN_c}{2\pi^2} \left\{ \ln[\Gamma(x_i)] - \frac{1}{2} \ln(2\pi) \right. \\ &\quad \left. + x_i - \frac{1}{2}(2x_i - 1) \ln(x_i) \right\}, \end{aligned} \quad (15)$$

$$\begin{aligned} \sigma_i^{\text{med}} &= \frac{M|q_i|eBN_c}{2\pi^2} \sum_{n_i=0}^{\infty} \alpha_{n_i} \int_0^{\infty} \frac{dp_z}{E_{ni}} \Theta(\tilde{\mu}_i - E_{ni}) \\ &= \frac{M|q_i|eBN_c}{2\pi^2} \sum_{n_i=0}^{n_i^{\text{max}}} \alpha_{n_i} \ln \left( \frac{\tilde{\mu}_i + \sqrt{\tilde{\mu}_i^2 - M_{ni}^2}}{M_{ni}} \right). \end{aligned} \quad (16)$$

The simple polynomial form for the Polyakov potential was improved by replacing the higher order polynomial term with the logarithm form [40,53,54]. At finite temperature, the following ansatz is suggested [55,56]

$$\begin{aligned} \mathcal{U}(\mu, \Phi) &= (a_0 T^4 + a_1 \mu^4 + a_2 T^2 \mu^2) \Phi^2 \\ &\quad + a_3 T_0^4 \ln(1 - 6\Phi^2 + 8\Phi^3 - 3\Phi^4). \end{aligned} \quad (17)$$

At zero temperature, we adopt the following formula

$$\mathcal{U}_0(\mu, \Phi) \equiv a_1 \mu^4 \Phi^2 + a_3 T_0^4 \ln(1 - 6\Phi^2 + 8\Phi^3 - 3\Phi^4), \quad (18)$$

where  $T_0 = 190$  MeV is very often used as the critical temperature for deconfinement in the PNJL model [57]. At zero temperature, the  $\mathcal{U}_0$  is importantly to the existence of confinement-deconfinement transition.

In literature, the four-quark vertex of one-gluon exchange diagram was changed into the entangled vertex [58]. Inspired by this phenomenology, the PNJL model was extended by introducing an entangled interaction between the quark condensate and the traced Polyakov loop in the EPNJL model [59], where the chiral restoration and the deconfinement transition is produced simultaneously in agreement with the Lattice result. Recently, the entanglement interaction dependent on the traced Polyakov loop in both the Polyakov potential and the effective interaction between quarks was introduced to avoid the lack of confinement physics in PNJL at  $T = 0$  [25]. In strong magnetic fields, we employ the phenomenology by making the scalar and vector interaction dependent on the traced Polyakov loop as

$$G_s \rightarrow G_s(1 - \Phi^2), \quad G_v \rightarrow G_v(1 - \Phi^2). \quad (19)$$

Therefore, the effective coupling interaction would vanish in the deconfined phase due to the dependence relation in Eq. (19).

At  $T = 0$ , the pressure is given by

$$P = -\mathcal{U}(\sigma, \rho, \mu, \Phi) + G_v \rho^2 - G_s \sigma^2 - \sum_{i=u,d} \Omega_i \quad (20)$$

with the Polyakov potential

$$\mathcal{U}(\sigma, \rho, \mu, \Phi) = \mathcal{U}_0(\mu, \Phi) - G_s \Phi^2 \sigma^2 + G_v \Phi^2 \rho^2. \quad (21)$$

From the thermodynamics potential one can easily obtain the quark number density  $\rho = \sum_{i=u,d} \rho_i$  with the  $i$  flavor contribution

$$\rho_i = \frac{3|q_i|eB}{2\pi^2} \sum_{n_i=0} \alpha_{n_i} \sqrt{\tilde{\mu}_i^2 - M_i^2 - 2n_i|q_i|eB}. \quad (22)$$

### III. NUMERICAL RESULT AND CONCLUSION

The important prediction of the QCD is the thermodynamic transition at sufficient high temperature and/or high density from the hadron phase to the color-deconfined quark-gluon plasma. The chiral transition and deconfinement transition is depicted by the well-defined order parameters. The quark condensate and the nonvanished Polyakov loop value are solved by the coupled gap equations as well as to minimize the thermodynamics potential. In this section our investigation of the QCD thermodynamics is restricted to the zero temperature. The four-fermion coupling interaction in the model is adopted with the fixed constant and magnetic field dependent running coupling in the following subsections respectively.

#### A. Results with fixed coupling constant

Being the nonrenormalizable model, a regularization procedure is usually applied by a three-momentum non-covariant cutoff  $\Lambda = 587.9$  MeV. The quark current mass as free parameters are adopted as  $m_u = m_d = 5.6$  MeV. The four-fermion couplings are  $G_s = 2.44/\Lambda^2$ , and  $G_v = 0.3G_s$ . We adopt the parameters as  $a_1 = -0.05$  and  $a_3 = -0.2$  for the confinement potential guided by the Ref. [25]. The presence of the vector interaction was discussed for the realization of the deconfinement transition at zero magnetic field. In this section, we would discuss the effect of the magnetic field on the deconfinement and chiral transition.

The dynamical mass is widely accepted as the order parameter of the chiral transition, which can be solved from the gap equation. In Fig. 1, the dynamical mass  $M$  for  $u$ - and  $d$ -quarks is shown as a function of the chemical potential  $\mu$ . The increases of the magnetic field is marked by the lines from the bottom  $0.2$  GeV<sup>2</sup> to the top  $0.6$  GeV<sup>2</sup>. It is clearly that in the chiral broken phase of small chemical potentials, the larger magnetic fields would result in larger dynamical masses. This catalyzing effect of magnetic field on the dynamical chiral symmetry breaking is known as the so-called MC effect [60]. In all the lines there is a sudden falling behavior, representing the appearance of the first-order phase transition from the chiral broken phase to the restoration. It should be emphasized that the chiral phase

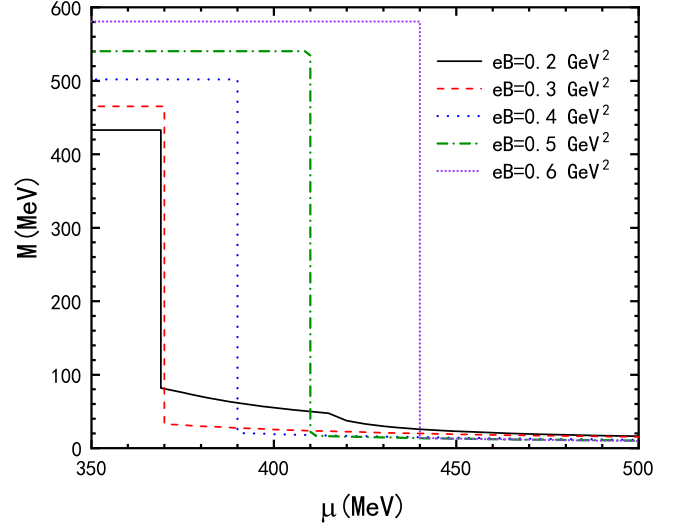


FIG. 1. The dynamical mass as a function of the chemical potential  $\mu$  for several magnetic fields  $eB$  in unit of GeV<sup>2</sup>.

transitions are always the first-order at zero temperature for various magnetic fields. The explicit chemical potential for the chiral restoration can be showed by the peak of the derivative of the  $M$  with respect to the chemical potential  $\mu$ . In Fig. 2, the susceptibility  $-\frac{dM}{d\mu}$  is shown as functions of the chemical potential. It is found that the peak of  $-\frac{dM}{d\mu}$  moves to the larger chemical potentials as the magnetic fields increase. It is again emphasized that the magnetic field has a strong tendency to enhance the quark-antiquark condensates, namely reflecting the MC effect at zero temperature.

In the above Figs. 1 and 2, the magnetic field is sufficiently large to suppress all the quarks to the LLL. The main contribution to the quark condensate should

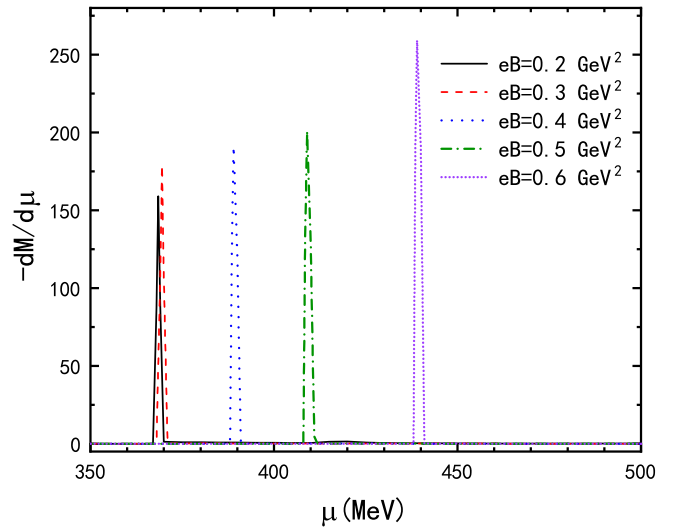


FIG. 2. The susceptibility  $-dM/d\mu$  as a function of chemical potential  $\mu$ , for several magnetic fields  $eB$  in unit of GeV<sup>2</sup>.

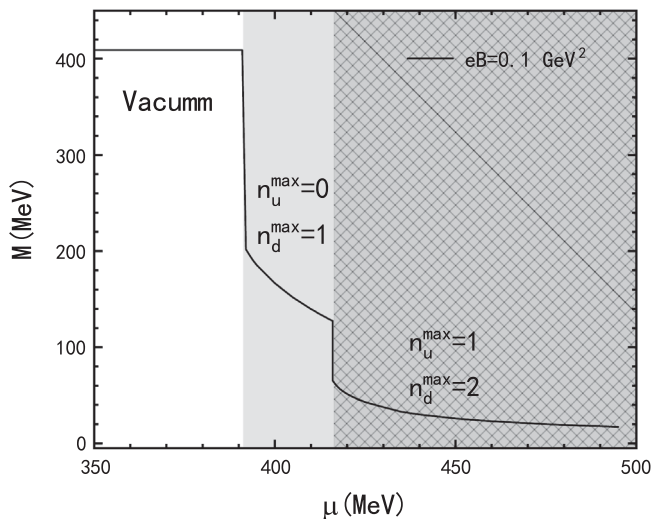


FIG. 3. The dynamical mass and the maximum Landau level as a function of chemical potential  $\mu$  at the magnetic field  $eB = 0.1 \text{ GeV}^2$ .

come from the quarks at the LLL. For the lowest nonzero value of  $|eB|$ , the zero Landau level occupation is not significant. The sum over more Landau level has to be taken. In Fig. 3, the dynamical mass is calculated at the  $eB = 0.1 \text{ GeV}^2$ . The two first-order transitions are resulted by the presence of a mismatch in the maximum Landau level for  $u$  and  $d$  quarks given by the  $n_u^{\max}$  and  $n_d^{\max}$ . It is clear that as the density increases, there are more Landau levels occupied by quarks but the  $n_d^{\max}$  is higher than  $n_u^{\max}$  in the weak magnetic field. It would have an influence on the trend of the magnetic catalysis on the critical chemical potential, which will be given in a later section.

In Fig. 4, the Polyakov loop  $\Phi$  as an order parameter of the deconfinement transition is shown versus the chemical

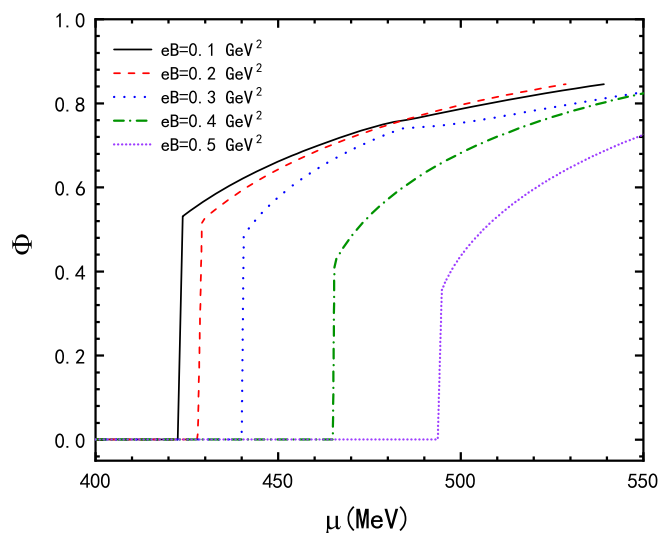


FIG. 4. The Polyakov loop  $\Phi$  as a function of chemical potential  $\mu$ , for several magnetic fields  $eB$  in unit of  $\text{GeV}^2$ .

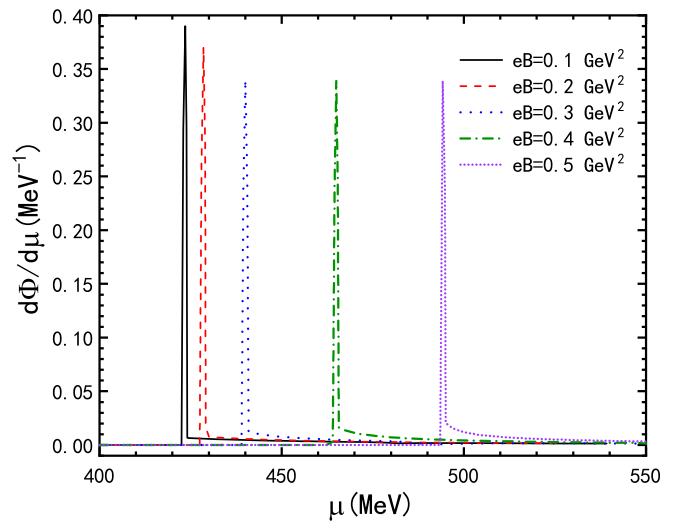


FIG. 5. The derivative of  $\Phi$  with respect to  $\mu$  as a function of chemical potential  $\mu$ , for several magnetic fields  $eB$  in unit of  $\text{GeV}^2$ .

potential at different magnetic fields. It is clearly seen that for all magnetic fields the values of  $\Phi$  have a sudden jump to around 0.5 from zero and then continue to increase as the magnetic field increases. This emphasized that there are first-order phase transitions from the confinement to the deconfined phases at zero temperature. A noteworthy point is the nonmonotonic behavior and the intersect with each other of the  $\Phi$  in the deconfined phase at low magnetic fields  $eB = 0.1, 0.2, \text{ and } 0.3 \text{ GeV}^2$ , which is caused by the Landau energy level. The Landau energy level is dominated by the values of dynamical mass  $M$ , chemical potential  $\mu$ , and the magnetic field. The value of the Landau energy level would more sensitively depend on the change of  $(M^2 - \mu^2)$  at the weak magnetic field.

Correspondingly, the derivative of  $\Phi$  with respect to the chemical potential  $\mu$  as a function of chemical potential  $\mu$  are shows in Fig. 5. The critical chemical potential  $\mu_c^\Phi$  can be exactly signaled by the peak of  $d\Phi/d\mu$ . It is worth noting that the deconfinement transition at zero temperature is produced in strong magnetic field in our model. Moreover, the first-order phase transition occurs in region of larger  $\mu_c^\Phi$  at more stronger magnetic field. This also implies a MC effect for the deconfinement transition.

## B. Results with magnetic-field-dependent coupling constant

Furthermore we discuss the results under the magnetic-field-dependent coupling constant. The coupling becomes weak at stronger magnetic fields due to the asymptotic freedom mechanism [61]. We chose the magnetic field-dependent coupling constant ansatz in Ref. [21,38]:

$$G_s(eB) = G_s^0 \frac{1 + a\left(\frac{eB}{\Lambda_{\text{QCD}}}\right)^2 + b\left(\frac{eB}{\Lambda_{\text{QCD}}}\right)^3}{1 + c\left(\frac{eB}{\Lambda_{\text{QCD}}}\right)^2 + d\left(\frac{eB}{\Lambda_{\text{QCD}}}\right)^4}. \quad (23)$$

In our work, the parameters are fixed as:  $\Lambda_{\text{QCD}} = 300$  MeV,  $a = 0.0108805$ ,  $b = -1.0133 \times 10^{-4}$ ,  $c = 0.02228$ ,  $d = 1.84558 \times 10^{-4}$  [21,38].

The critical chemical potentials for the chiral and deconfinement phase transitions are plotted as the functions of  $eB$  with two kinds of couplings in Fig. 6. The blue lines on the left panel show the results  $\mu_c^\chi$  of the chiral phase transitions. According to the statement in the preceding section, there are two first-order transitions at  $eB = 0.1$  GeV<sup>2</sup>. The average of two chemical potentials is taken as the critical chemical potential that plotted in Fig. 6. It is obvious that at the fixed coupling  $G_s$  the critical chemical potential marked by the blue-dashed line is decreased first and then goes up as the magnetic field increases. There is a clear qualitative similarity with the results in Refs. [21,60,62]. In the region of sufficiently small magnetic fields and larger coupling constant, the critical chemical potential decreases with the field in Fig. 6 from Ref. [60]. And in the weak magnetic field regime, the critical chemical potential would show a temporary decrease as the magnetic field increases at  $T = 0$  in Fig. 7.4 of Ref. [62]. However, as the magnetic field goes up to much larger value, the magnetic catalysis effect on the chiral chemical potential becomes obvious. By employing the running coupling interaction  $G_s(eB)$ , the  $\mu_c^\chi$  marked by the blue-solid line would go down drastically. This shows a visible difference between the two kinds of interactions. The trend of  $\mu_c^\chi$  with  $eB$  indicates the so-called IMC effect, which was realized by the behavior of the decreasing critical temperature as the  $eB$  increases [63]. The magnitude of decrease of  $\mu_c^\chi$  is almost qualitatively in agreement

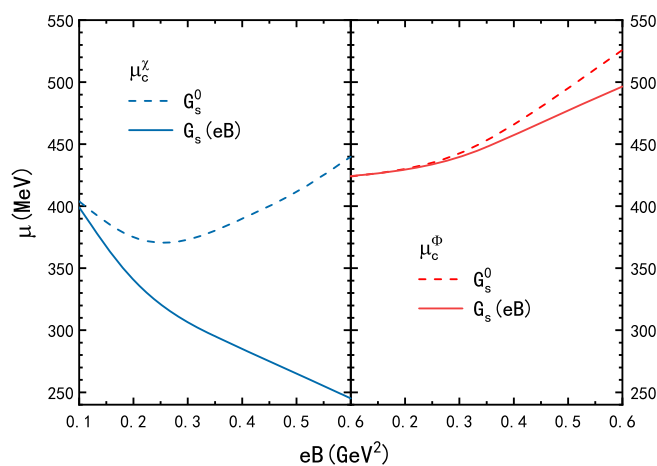


FIG. 6. The critical chemical potentials of chiral (left panel) and deconfinement phase transitions (right panel) as the function of  $eB$ , with a constant coupling  $G_s^0$  and a magnetic field dependent coupling  $G_s(eB)$  from Eq. (23).

with the results in Ref. [21] at zero temperature. On the right panel, the critical chemical potential  $\mu_c^\Phi$  depicted by the red lines is steadily growing as the magnetic field increases under the both couplings  $G_s^0$  and  $G_s(eB)$ . It can be seen that the magnetic field dependence of the coupling  $G_s(eB)$  in Eq. (23) would have weak influence on the deconfinement transition. It illustrates that the deconfinement transition depends insensitively on the running behavior of the coupling constant. The trend of  $\mu_c^\Phi$  always keeps a monotonical increasing function. On the contrary, it is also observed that for the chiral transition, the difference in  $\mu_c^\chi$  between the couplings  $G_s(eB)$  and  $G_s$  becomes larger as the magnetic field increases, which indicates that the chiral restoration is more sensitive to the strength of the applied magnetic field through the scalar interaction.

In literature, the quarkyonic phase was proposed as a new phase of QCD and expected to exist at large chemical potentials in the chiral symmetry restoration but confined region [64–68], which indicates that the chiral restoration transition occurs earlier than the deconfinement transition as the chemical potential increases. To facilitate this observation, the critical chemical potential for the chiral phase transition and the deconfinement phase transition are compared in Fig. 7. Results with a fixed coupling constant  $G_s$  are shown on left panel and with a magnetic-field-dependent coupling constant  $G_s(eB)$  on right panel. The critical chemical potential  $\mu_c^\chi$  with both couplings  $G_s$  and  $G_s(eB)$  are always lower than the  $\mu_c^\Phi$  for the deconfinement phase transition. Consequently, there is a region  $\mu_c^\chi < \mu < \mu_c^\Phi$  is identified as the quarkyonic phase, where the chiral symmetry is partial restored while quarks are still confined. It can be seen that the quarkyonic phase window marked by the gray region is enlarged as the magnetic field increases. Moreover, by comparison with the fixed coupling  $G_s$ , the magnetic-field-dependent coupling

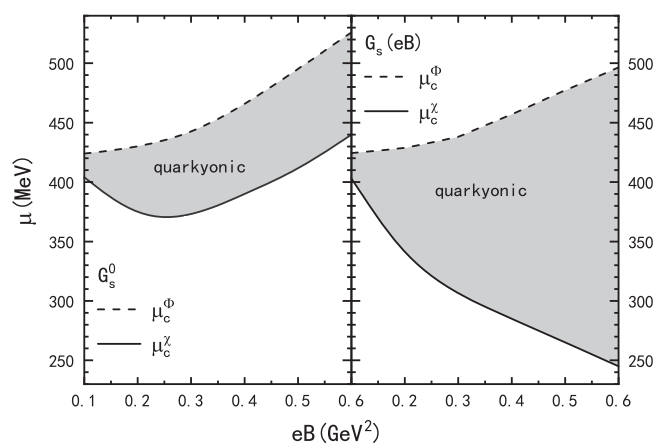


FIG. 7. The critical chemical potentials  $\mu_c^\chi$ ,  $\mu_c^\Phi$ , and the possible quarkyonic phase window at zero temperature in strong magnetic fields, with a constant coupling  $G_s^0$  (left panel) and a magnetic field dependent coupling  $G_s(eB)$  (right panel).

constant  $G_s(eB)$  on the right panel would lead to a larger expansion of the quarkyonic window at stronger magnetic fields.

#### IV. SUMMARY

In this paper, we have investigated the deconfinement phase transition and chiral phase transition at zero temperature by improving the PNJL0 model to the strong magnetic field. The interaction of quarks is described by the Polyakov potential together with the entanglement of the scalar and vector interactions. The chiral restoration and the deconfinement transitions take place as the chemical potential increases. The strong magnetic field would play an important role in the phase transition. It has been found that the critical chemical potential for the deconfinement moves to the larger value as the magnetic field increase, which indicate the MC effect no matter how the coupling constant is employed. Moreover, the critical chemical potential  $\mu_c^\Phi$  becomes more insensitive to the magnetic field under the running coupling  $G(eB)$ . In contrary, the effect of the magnetic field on the chiral restoration would sensitively depend on the coupling.

At larger magnetic fields, it has been shown that the MC effect with the magnetic-field independent coupling  $G_s$  would convert to the IMC with the running coupling  $G_s(eB)$ . Finally, it has been verified that the quarkyonic phase window is present under the condition  $\mu_c^\chi < \mu_c^\Phi$ , where the chiral symmetry is restored but the quarks are still confined. Moreover, the quarkyonic phase window is evidently enlarged by the running coupling  $G_s(eB)$  at stronger magnetic fields. Since the previous phenomenological model mainly concentrate on the knowledge of QCD at finite temperature, we expect that our work at zero temperature can be regarded as a complementary to the QCD diagram, where the critical chemical potential would be important to the dense star matter.

#### ACKNOWLEDGMENTS

The authors would like to thank support from the National Natural Science Foundation of China under the Grants No. 11875181, No. 11705163, and No. 12147215. This work was also sponsored by the Fund for Shanxi “1331 Project” Key Subjects Construction.

- 
- [1] S. Leupold, K. Redlich, M. Stephanov, A. Andronic, D. Blaschke, M. Bluhm, A. Dumitru, Z. Fodor, B. Friman, C. Fuchs *et al.*, *Lect. Notes Phys.* **814**, 39 (2011).
  - [2] K. Fukushima and T. Hatsuda, *Rep. Prog. Phys.* **74**, 014001 (2011).
  - [3] M. D’Elia, F. Manigrasso, F. Negro, and F. Sanfilippo, *Phys. Rev. D* **98**, 054509 (2018).
  - [4] G. S. Bali, F. Bruckmann, G. Endrodi, Z. Fodor, S. D. Katz, S. Krieg, A. Schafer, and K. K. Szabo, *J. High Energy Phys.* **02** (2012) 044.
  - [5] S. Ejiri, *Phys. Rev. D* **69**, 094506 (2004); K. Splittorff, *Proc. Sci.*, LAT2006 (2006) 023 [arXiv:hep-lat/0610072]; K. Splittorff and J. J. M. Verbaarschot, *Phys. Rev. Lett.* **98**, 031601 (2007).
  - [6] A. Ayala, C. A. Dominguez, S. Hernandez-Ortiz, L. A. Hernandez, M. Loewe, D. M. Paret, and R. Zamora, *Phys. Rev. D* **98**, 031501(R) (2018).
  - [7] C. J. Xia, G. X. Peng, T. T. Sun, W. L. Guo, D. H. Lu, and P. Jaikumar, *Phys. Rev. D* **98**, 034031 (2018).
  - [8] J. F. Xu, D. B. Kang, G. X. Peng, and C. J. Xia, *Chin. Phys. C* **45**, 015103 (2021).
  - [9] X. J. Wen, X. H. Zhong, G. X. Peng, P. N. Shen, and P. Z. Ning, *Phys. Rev. C* **72**, 015204 (2005).
  - [10] E. J. Ferrer, V. dela Incera, I. Portillo, and M. Quiroz, *Phys. Rev. D* **89**, 085034 (2014).
  - [11] P. Costa, M. Ferreira, H. Hansen, D. P. Menezes, and C. Providência, *Phys. Rev. D* **89**, 056013 (2014).
  - [12] Y. Nambu and G. Jona-Lasinio, *Phys. Rev.* **122**, 345 (1961).
  - [13] Y. Nambu and G. Jona-Lasinio, *Phys. Rev.* **124**, 246 (1961).
  - [14] M. Buballa, *Phys. Rep.* **407**, 205 (2005).
  - [15] U. Vogl and W. Weise, *Prog. Part. Nucl. Phys.* **27**, 195 (1991).
  - [16] S. P. Klevansky, *Rev. Mod. Phys.* **64**, 649 (1992).
  - [17] A. Chodos, R. L. Jaffe, K. Johnson, C. B. Thorn, and V. F. Weisskopf, *Phys. Rev. D* **9**, 3471 (1974).
  - [18] A. Chodos, R. L. Jaffe, K. Johnson, and C. B. Thorn, *Phys. Rev. D* **10**, 2599 (1974).
  - [19] T. A. DeGrand, R. L. Jaffe, K. Johnson, and J. E. Kiskis, *Phys. Rev. D* **12**, 2060 (1975).
  - [20] C. Sasaki, B. Friman, and K. Redlich, *Phys. Rev. D* **75**, 074013 (2007).
  - [21] M. Ferreira, P. Costa, and C. Providência, *Phys. Rev. D* **97**, 014014 (2018).
  - [22] M. Biswal, S. Digal, and P. S. Saumia, *Phys. Rev. D* **102**, 074020 (2020).
  - [23] J. P. Carlomagno and M. F. Izzo. Villafañe, *Phys. Rev. D* **100**, 076011 (2019).
  - [24] S. Mao, *Phys. Rev. D* **97**, 011501(R) (2018).
  - [25] O. A. Mattos, T. Frederico, and O. Loureno, *Eur. Phys. J. C* **81**, 24 (2021).
  - [26] O. A. Mattos, T. Frederico, C. H. Lenzi, M. Dutra, and O. Lourenço, *Phys. Rev. D* **104**, 116001 (2021).
  - [27] V. Skokov, A. Y. Illarionov, and V. Toneev, *Int. J. Mod. Phys. A* **24**, 5925 (2009).
  - [28] G. Chanmugam, *Annu. Rev. Astron. Astrophys.* **30**, 143 (1992).
  - [29] D. Lai, *Rev. Mod. Phys.* **73**, 629 (2001).
  - [30] V. Dexheimer, B. Franzon, R. O. Gomes, R. L. S. Farias, S. S. Avancini, and S. Schramm, *Phys. Lett. B* **773**, 487 (2017).

- [31] D. E. Kharzeev, L. D. McLerran, and H. J. Warringa, *Nucl. Phys.* **A803**, 227 (2008).
- [32] T. Vachaspati, *Phys. Lett. B* **265**, 258 (1991).
- [33] D. Grasso and H. R. Rubinstein, *Phys. Rep.* **348**, 163 (2001).
- [34] V. P. Gusynin, V. A. Miransky, and I. A. Shovkovy, *Phys. Rev. Lett.* **73**, 3499 (1994).
- [35] R. L. S. Farias, K. P. Gomes, G. I. Krein, and M. B. Pinto, *Phys. Rev. C* **90**, 025203 (2014).
- [36] R. L. S. Farias, V. S. Timoteo, S. S. Avancini, M. B. Pinto, and G. Krein, *Eur. Phys. J. A* **53**, 101 (2017).
- [37] A. Ahmad and A. Raya, *J. Phys. G* **43**, 065002 (2016).
- [38] M. Ferreira, P. Costa, O. Lourenço, T. Frederico, and C. Providência, *Phys. Rev. D* **89**, 116011 (2014).
- [39] H. Hansen, W. M. Alberico, A. Beraudo, A. Molinari, M. Nardi, and C. Ratti, *Phys. Rev. D* **75**, 065004 (2007).
- [40] S. Rossner, C. Ratti, and W. Weise, *Phys. Rev. D* **75**, 034007 (2007).
- [41] M. Dutra, O. Lourenço, A. Delfino, T. Frederico, and M. Malheiro, *Phys. Rev. D* **88**, 114013 (2013).
- [42] J. S. Schwinger, *Phys. Rev.* **82**, 664 (1951).
- [43] D. Ebert, K. G. Klimenko, M. A. Vdovichenko, and A. S. Vshivtsev, *Phys. Rev. D* **61**, 025005 (1999).
- [44] A. Ayala, C. A. Dominguez, L. A. Hernandez, M. Loewe, A. Raya, J. C. Rojas, and C. Villavicencio, *Phys. Rev. D* **94**, 054019 (2016).
- [45] R. A. Abramchuk, M. A. Andreichikov, Z. V. Khaidukov, and Y. A. Simonov, *Eur. Phys. J. C* **79**, 1040 (2019).
- [46] D. P. Menezes, M. B. Pinto, S. S. Avancini, A. P. Martinez, and C. Providencia, *Phys. Rev. C* **79**, 035807 (2009).
- [47] S. S. Avancini, D. P. Menezes, and C. Providencia, *Phys. Rev. C* **83**, 065805 (2011).
- [48] D. P. Menezes, M. Benghi Pinto, S. S. Avancini, and C. Providencia, *Phys. Rev. C* **80**, 065805 (2009).
- [49] P. G. Allen and N. N. Scoccola, *Phys. Rev. D* **88**, 094005 (2013).
- [50] R. L. S. Farias, K. P. Gomes, G. Krein, and M. B. Pinto, *J. Phys. Conf. Ser.* **630**, 012046 (2015).
- [51] A. Rabhi and C. Providencia, *Phys. Rev. C* **83**, 055801 (2011).
- [52] B. Chatterjee, H. Mishra, and A. Mishra, *Phys. Rev. D* **84**, 014016 (2011).
- [53] K. Fukushima, *Phys. Lett. B* **591**, 277 (2004).
- [54] S. Roessner, T. Hell, C. Ratti, and W. Weise, *Nucl. Phys.* **A814**, 118 (2008).
- [55] V. A. Dexheimer and S. Schramm, *Nucl. Phys.* **A827**, 579C (2009).
- [56] V. A. Dexheimer and S. Schramm, *Phys. Rev. C* **81**, 045201 (2010).
- [57] C. Ratti, M. A. Thaler, and W. Weise, *Phys. Rev. D* **73**, 014019 (2006).
- [58] K. I. Kondo, *Phys. Rev. D* **82**, 065024 (2010).
- [59] Y. Sakai, T. Sasaki, H. Kouno, and M. Yahiro, *Phys. Rev. D* **82**, 076003 (2010).
- [60] V. A. Miransky and I. A. Shovkovy, *Phys. Rep.* **576**, 1 (2015).
- [61] S. R. Coleman and D. J. Gross, *Phys. Rev. Lett.* **31**, 851 (1973).
- [62] M. R. B. Ferreira, Ph.D. thesis, QCD phase diagram under an external magnetic field, 2015, <https://inspirehep.net/literature/1501993>.
- [63] F. Preis, A. Rebhan, and A. Schmitt, *J. High Energy Phys.* **03** (2011) 033.
- [64] S. Mao, Y. Wu, and P. Zhuang, *J. Phys. Soc. Jpn. Conf. Proc.* **20**, 011009 (2018).
- [65] K. Fukushima, *Phys. Rev. D* **77**, 114028 (2008).
- [66] H. Abuki, R. Anglani, R. Gatto, G. Nardulli, and M. Ruggieri, *Phys. Rev. D* **78**, 034034 (2008).
- [67] L. McLerran, K. Redlich, and C. Sasaki, *Nucl. Phys.* **A824**, 86 (2009); Y. Hidaka, L. McLerran, and R. D. Pisarski, *Nucl. Phys.* **A808**, 117 (2008).
- [68] F. Buisseret and G. Lacroix, *Phys. Rev. D* **85**, 016009 (2012).